

# Understanding the Incipient Discharge Activity with Epoxy/MoS<sub>2</sub> Nanocomposites

P. NAGACHANDRIKA\*, K. SRIDHARAN\*, R. SARATHI\* and Noboru YOSHIMURA\*\*

\* Department of Electrical Engineering, IIT Madras, Chennai 600 036, India

\*\* Tohoku University of Community Service and Science, Yamagata 998-8580, JAPAN

E-mail: rsarathi@iitm.ac.in

In power apparatus, it is essential to have insulating material with high resistance to damages. MoS<sub>2</sub> nanofiller can provide good mechanical, insulating and thermal properties. An attempt has been made to understand the resistance to damage of the material through surface discharge studies and it has been observed that addition of low weight percentage of MoS<sub>2</sub> has high resistance to surface discharges. The results are aided by surface charge accumulation studies. Characteristic variation in dielectric properties of the material indicates that low weight percentage addition of MoS<sub>2</sub> nanofillers shows a reduction in permittivity of the material and has low loss. It was observed that epoxy nanocomposites are resistant to water droplet initiated discharges. Corona inception voltage (CIV) with multiple droplets, droplet near high voltage and ground electrode were measured. It is interesting to note that, irrespective of the number or the position of water droplets and voltage profile, 0.5 wt% MoS<sub>2</sub> added epoxy shows high resistance to discharges. It was also observed that CIV reduces when two droplets placed in electrode gap and when the droplet is placed near the electrodes. Glass transition temperature ( $T_g$ ) of epoxy/MoS<sub>2</sub> varies with filler loading. Optical emission spectroscopy (OES) results indicate that the plasma temperature is low for epoxy resin with 0.5 wt% MoS<sub>2</sub>.

**Keywords :** Nanocomposite, surface discharge, MoS<sub>2</sub>, surface roughness, surface charge accumulation, epoxy resin

## 1 INTRODUCTION

Epoxy resin is basically a high-performance material and is used as an insulant in all high voltage power apparatus because of its high electrical, thermal and mechanical properties. With the advancement of nano materials, its use as filler has provided greater advantage to achieve required electrical, thermal and mechanical properties [1, 2]. Carbon nanotubes (CNT) and graphene have good application to use as an electric field grading material [3]. Recently, MoS<sub>2</sub> material is gaining popularity because of its inherent characteristics of high band gap which will not impart electrical conductivity and the world over researchers have indicated that addition of it as filler content can enhance mechanical and thermal properties of the material [4]. In power apparatus, surface discharge activity is one of the mechanisms by which the solid insulation fails. The surface resistivity and hydrophobicity of the material play an important role on life of insulating material. The surface charge accumulation can enhance the tangential electric field, leading to surface discharge activity and poor hydrophobicity of the material, which lead to thinning of water droplet causing inception of corona activity near the water droplet edge. The characteristic variation in degradation of insulating material occurs due to enhancement of local electric field and hence it has become important to ensure the surface free from charge accumulation/electric field enhancement in the insulating material. Conventionally, the inorganic fillers, namely, silicon

carbide material is used as a filler material in epoxy resin, which can relieve the accumulated charge, because of its semiconducting properties. In recent times, the molybdenum di-sulphide material, is gaining importance because of its inherent material properties and can be alternative material because of its semi-conductive nature [5].

Under normal operating conditions, the insulating material may expose to electrical discharges due to surface discharges or degradation of insulating materials due to corona activity. These discharges in turn can cause degradation of the insulating material over a period thereby alternating the fundamental properties of insulating material thereby reducing the life of the equipment [6]. Therefore, there is a strong need for developing electrical insulating materials possessing good discharge resistant characteristics. Recently, CIGRE working group has indicated development of non-standard materials for improved performance [7].

Epoxy resin with silicon carbide reinforcement exhibits good partial discharge resistance characteristics [8]. In the electric power sector, it is generally utilized as stress grading substance for high voltage electrical machines [9, 10]. Many studies have reported the use of non-linear dielectrics in power apparatus operating at normal ambient temperatures [11]. A major problem with insulating material is moisture condensation forming water droplet. If a water droplet is sitting on the top of insulating material, under high electric field, corona activity incets followed with surface discharge activity, causing surface temperature rise followed

with carbonization of surface. Thus, it is essential to understand the discharge behavior due to water droplet sitting on insulation surface and surface damage due to arcing process.

Having known all this, in the present work, an attempt has been made to understand the following important aspects. (i) Variation in surface discharge inception voltage (SDIV) in epoxy MoS<sub>2</sub> nanocomposites material under AC and DC voltages using IEC (b) electrode configuration, (ii) Variation in fundamental properties of material including relative permittivity, tan δ, contact angle and surface roughness of the epoxy molybdenum disulphide nanocomposites (iii) To understand the influence of water droplet on corona inception, its local temperature by optical emission studies and the analysis of electromagnetic waves generated during corona activity by adopting UHF technique.

## 2 EXPERIMENTAL STUDIES

### 2.1 Sample Preparation

In the present work, the required quantity of nano molybdenum disulfide material is mixed with ethanol by ultrasonic mixing and added to epoxy resin. The epoxy resin added nano filler solution subjected to high-speed shear mixing (rotation speed 4000 rpm) and ultra-sonication (frequency - 20 kHz) for 1 h and 4 h, respectively. On completion of sonication process, tri-ethylene tetra-amine (TETA) hardener was added to the nanoparticle dispersed epoxy resin and casted into a sheet plate of required dimension and degassed. In the present work, epoxy nanocomposites with 0.25, 0.5, 1 and 5 wt% of nano-molybdenum disulfide were prepared with a dimension 30 × 30 × 1 mm.

The hydrophobicity of the material analyzed through contact angle measurement and the dielectric properties of the material especially the permittivity and tan δ measured by using Novo control technology broadband dielectric/impedance spectrometer (Alpha-A High-performance frequency analyzer) in the frequency range of 10<sup>-1</sup> Hz to 10<sup>6</sup> Hz, at different temperatures.

The hydrophobic property of the material analyzed by measure of static contact angle measurement by liquid droplet method [12]. The volume of water used for the study is about 20 μl. The contact angle was measured using the following equation,

$$\theta = 2 \tan^{-1} \left( \frac{2h}{d} \right) \quad \dots \dots \dots (1)$$

where *d* is the diameter of a liquid drop and *h* is the height of the liquid drop. For each sample, contact angle was measured at six various positions and averaged.

The thermal properties were studied by using differential scanning calorimeter (DSC) of M/s Netzsch DSC200 F3 Maia. The DSC heating curves of all the samples were obtained for a temperature range from -300°C to 1000°C in a nitrogen atmosphere. The heating rate was fixed at 10°C/min.

### 2.2 Surface Discharge Studies

Figure 1 depicts the schematic of the experimental setup for surface discharge studies using IEC (b) electrode [13]. The top IEC electrode connected to high voltage and the bottom electrode is flat circular electrode. A 1 mm thick × 5 cm diameter circular epoxy nanocomposite specimen was placed on the bottom plane electrode. The top rod electrode of 6 mm radius (IEC (b) electrode) was connected to the high voltage and the tip of the electrode was made to just touch the nanocomposite sheet. Surface discharge incepts at the triple point junction formed at the edge of top high

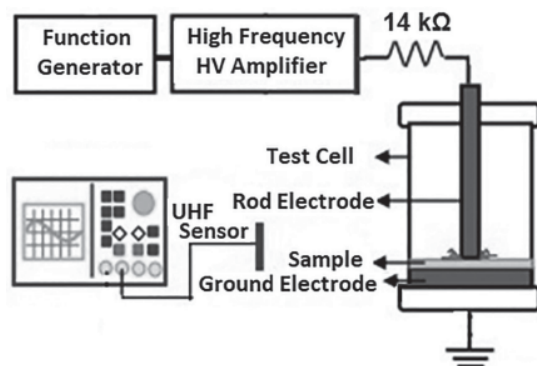


Figure 1 Experimental set-up for surface discharge.

voltage electrode touching the nanocomposite specimen and the surrounding medium. The radiated signal due to surface discharge/corona activity is identified by using UHF non-directional sensors. The applied high AC/DC voltages are generated by use of a Trek amplifier (model 20/20A) with its input from the function generator. The applied AC/DC voltage was measured using Tektronix high voltage probe.

### 2.3 Corona Discharge Activity with water droplet

The experimental setup used for understanding corona discharge activity due to water droplet adopting IEC 60112 electrode configuration is shown in Figure 2 [14].

Figure 3 depicts the test electrodes used in the present study. The electrodes were separated by a distance of 30 mm. One electrode was connected to the high voltage source and the other electrode was connected to the ground. The radiated electromagnetic waves formed due to corona activity identified by use of UHF sensor. The frequency response of the sensor is shown in Figure 4 [15].

The optical light emitted during corona/discharge activity is

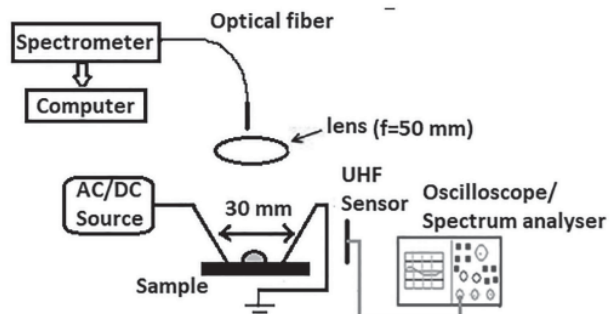


Figure 2 Experimental set-up for corona discharge.



Figure 3 Test electrode arrangement

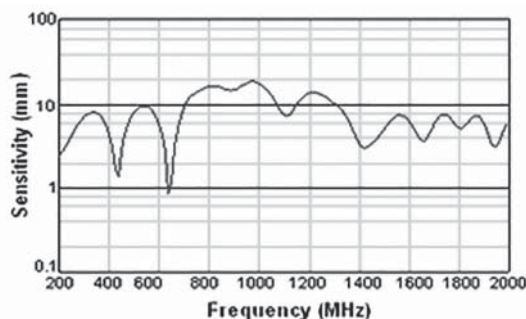


Figure 4 Frequency response of the UHF sensor.

analyzed using optical emission spectrometer, to understand composition of material and the local temperature during arcing formed by water droplet, under high electric fields. Optical emission during discharge on the material is focused using a lens with a focal length of 50 mm and it is coupled to a spectrometer (190 to 1035 nm, Tech5) with an NMOS linear image sensor (S3901, Hamamatsu) using a multimode optical fiber with a core diameter of 600  $\mu\text{m}$ , 0.32 numerical aperture (NA).

#### 2.4 Surface Charge Measurement

The decay characteristics of the charges deposited by the corona discharge process were analyzed by using electrostatic voltmeter (Figure 5) [16]. The gap distance between the sensor (with cross-section area ( $A$ )) and the surface of the charge deposited specimen ( $d$ ) was maintained at 2 mm. This gap distance allows covering the charge present up to a radius of 5 mm on the surface of the specimen. The charge ( $Q$ ) on the surface of epoxy-MoS<sub>2</sub> nanocomposites was calculated as,

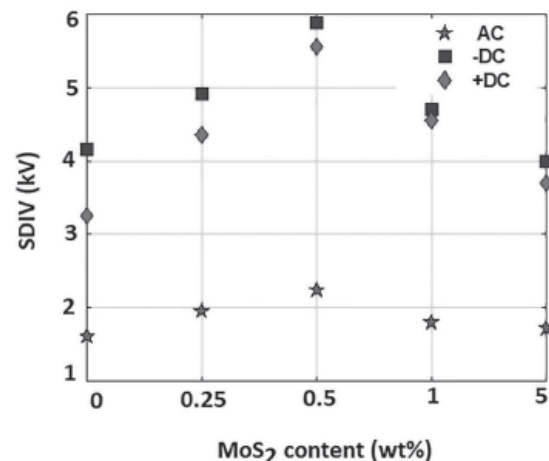
$$Q = V \frac{\epsilon_0 \epsilon_r A}{d} \quad \dots \dots \dots (2)$$

Where,  $\epsilon_0$  and  $\epsilon_r$  are the relative permittivity of vacuum and of the medium, respectively.

### 3 RESULTS AND DISCUSSIONS

#### 3.1 Surface Discharge Inception Voltage (SDIV)

Figure 6 shows characteristic variation in surface discharge inception voltage with epoxy nanocomposites containing MoS<sub>2</sub> content with different weight percentages. The surface discharge inception voltages were measured based on the first pulse being captured by the oscilloscope from the UHF sensor output. It is observed that, when wt% of MoS<sub>2</sub> in epoxy resin increased above certain limit, a reduction in surface discharge inception voltage is observed. Raised inception voltage at lower nanofiller loadings can be attributed to the barrier effect of the nanofiller present in the matrix. When the wt% of MoS<sub>2</sub> is increased, agglomeration of

Figure 6 Surface discharge inception voltage variations with respect to the concentration of MoS<sub>2</sub>.

nano fillers occurs and the material performance will be with micro fillers. Hence, uniform dispersion of nano filler is one of the basic requirements, to achieve the desired properties of the material.

To understand the hydrophobicity of the material, contact angle was measured and is shown in Figure 8. It is observed that above certain wt% of MoS<sub>2</sub>, a reduction in contact angle occurs. To understand the damage caused due to discharge activity, surface roughness of the material is measured. The variation in surface roughness with MoS<sub>2</sub> is shown in Figure 9. The discharge exposed composites show a decrement in surface roughness with increasing in wt% of MoS<sub>2</sub>.

Highly roughened surfaces have lower contact angle. In the process, when the high voltage electrode is in contact with the rough surface, the air gap formed due to rough surface, at the interface of high voltage electrode and the insulating material, the electric field concentration be high thereby initiating incipient discharges causing carbonization of the surface. In the process, charges gets accumulated at the carbonized zone enhancing surface discharge activity and a sustained surface discharge activity prevails at just lower voltages confirming surface roughness and surface discharge inception voltage have inverse relationship. Hence the contact angle and SDIV are directly correlated.

#### 3.2 Surface Charge Measurement

Figure 7 shows charge decay of epoxy molybdenum disulfide nanocomposites. The charge decay characteristics predominates on increase of MoS<sub>2</sub> concentration in epoxy resin. It is mainly because that the MoS<sub>2</sub> has large electronegativity [17], due to which it captures charges and forms a shield. The charges captured in this shielding layer generate an internal field opposite to the applied field, which decreases effective electric field strength thereby reducing the charges injected into the bulk.

#### 3.3 Dielectric Properties

Figure 10 and 11 show the relative permittivity and the tan $\delta$  plots of epoxy nanocomposites in the frequency range of 0.1 Hz to  $10^6$  Hz. It is observed that the effective permittivity of all nanocomposites decreases with increase the frequency of supply. The cause for it is due to the fact, at low frequencies, dipolar group present in the composite material can orient themselves causing increased permittivity. At higher frequencies, the response time of

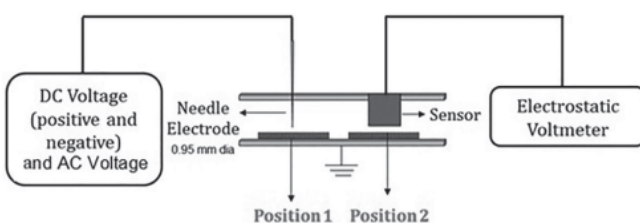


Figure 5 Surface charge measurement set-up.

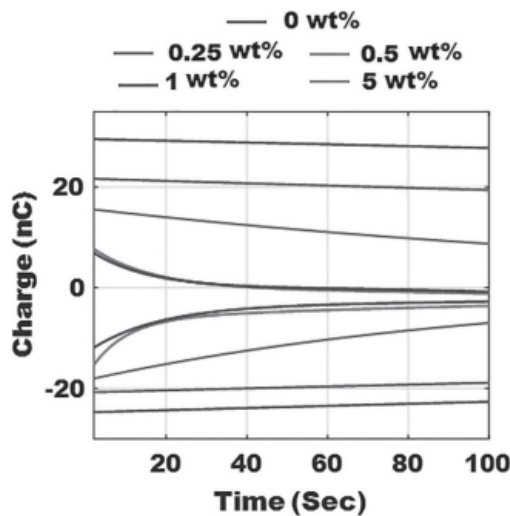


Figure 7 Surface charge characteristics of epoxy nanocomposites with increase in filler concentration.

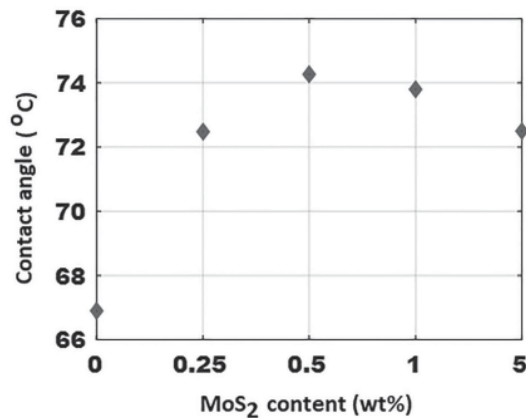


Figure 8 Contact angle variation with respect to the concentration of  $\text{MoS}_2$ .

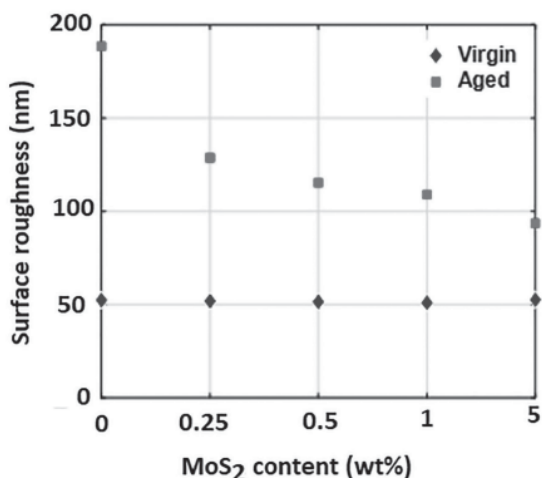


Figure 9 Variation of surface roughness with respect to the concentration of  $\text{MoS}_2$ .

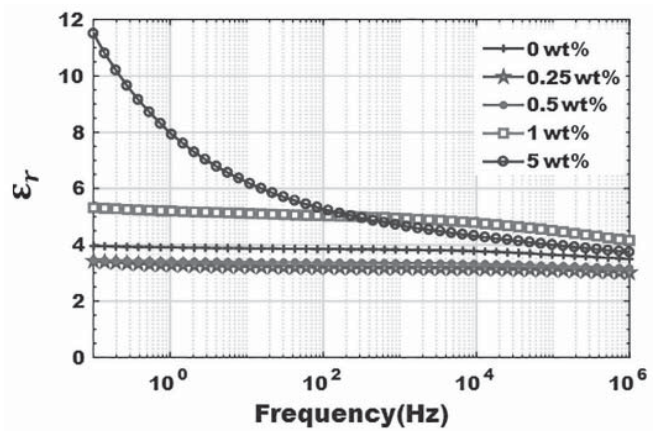


Figure 10 Variations in relative permittivity with frequency at 30°C.

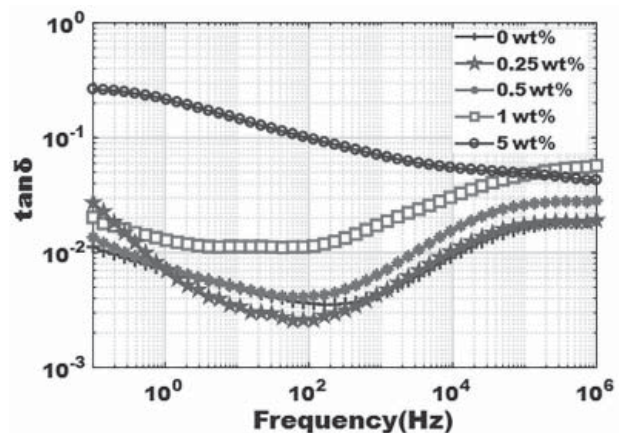


Figure 11 Variation in  $\tan \delta$  of epoxy nanocomposites with frequency at 30°C.

the dipolar material is low causing permittivity low. In addition, the intrinsic permittivity of nanofiller decreases with increase in supply frequency [18]. It is observed that  $\tan \delta$  values of all epoxy nanocomposites (except 5 wt%) decrease with increase in frequency upto 100 Hz, and then starts increasing with further increment in frequency. Such characteristics are also observed by other researchers [19].

### 3.4 Water Droplet Initiated Discharges

Figure 12 shows variation in corona inception voltage caused due to water droplet on  $\text{MoS}_2$  material, under AC and DC voltages. It can be observed that corona inception voltage increases up to 0.5 wt%  $\text{MoS}_2$  added epoxy, and then it decreases irrespective of voltage profile and the position of the droplet. Figure 13 (i) and 13(ii) shows the variation in corona inception voltage with water droplet on pure epoxy resin and with 0.5 wt%  $\text{MoS}_2$  added epoxy nanocomposites respectively. It is observed that the CIV decreases when two droplets placed in electrode gap. The decrement in CIV is more for two droplets than droplet near HV or ground electrode. This could be due to shape variation in droplets on application of voltage, which enhances local electric field, causing discharges to occur at lower voltages. The corona inception voltage when the droplet is near HV and ground electrode is almost same.

Figure 14 shows the variation in corona inception voltage due to water droplet on epoxy nanocomposites under high frequency

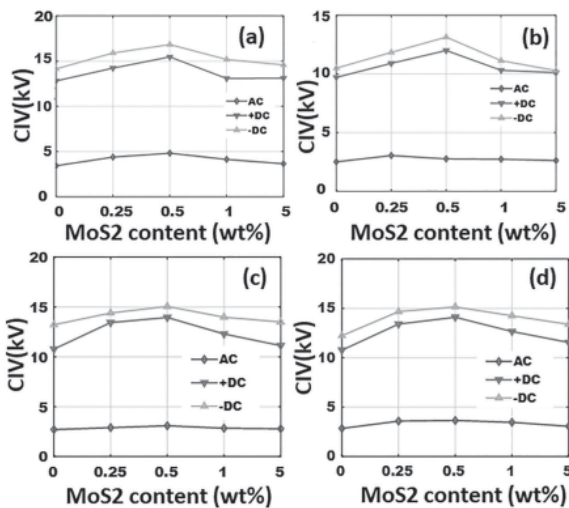


Figure 12 Corona inception voltage when (a) single droplet, (b) two droplet in electrode gap, (c) a droplet near high voltage electrode, (d) a droplet near ground electrode.

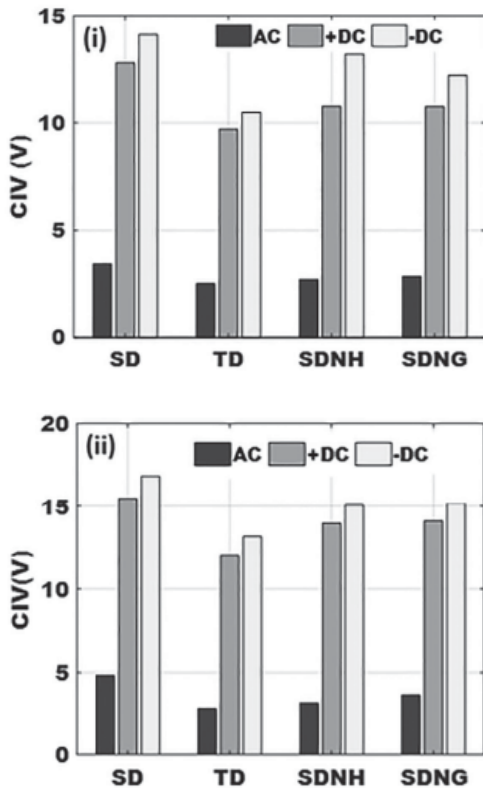


Figure 13 Corona inception voltage of pure epoxy for different profiles, (i) Pure epoxy, (ii) 0.5 wt% MoS<sub>2</sub> added epoxy. (SD-single droplet, TD- two droplets, SDNH-single droplet near HV, SDNG-single droplet near ground electrode).

AC voltages. It is observed that corona inception voltage increases with increase in the frequency of supply voltage. From Figure 14, it is clear that corona inception voltage increases with increase in frequency of supply voltage for pure, 0.5 and 5 wt% MoS<sub>2</sub> added epoxy samples. Figure 15 shows the characteristic variation in corona inception voltage due to water droplet of different conductivity on epoxy MoS<sub>2</sub> nanocomposites under AC, DC voltages. Irrespective of the conductivity of droplet, corona

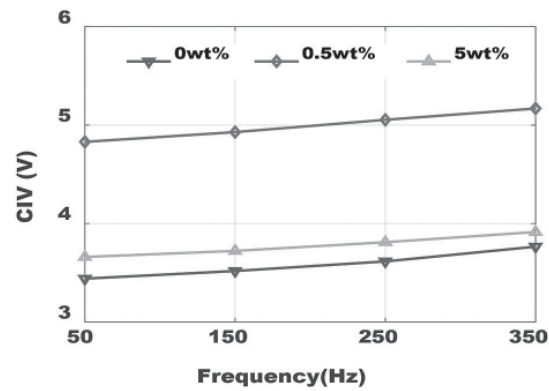


Figure 14 Corona inception voltage of samples at different frequencies.

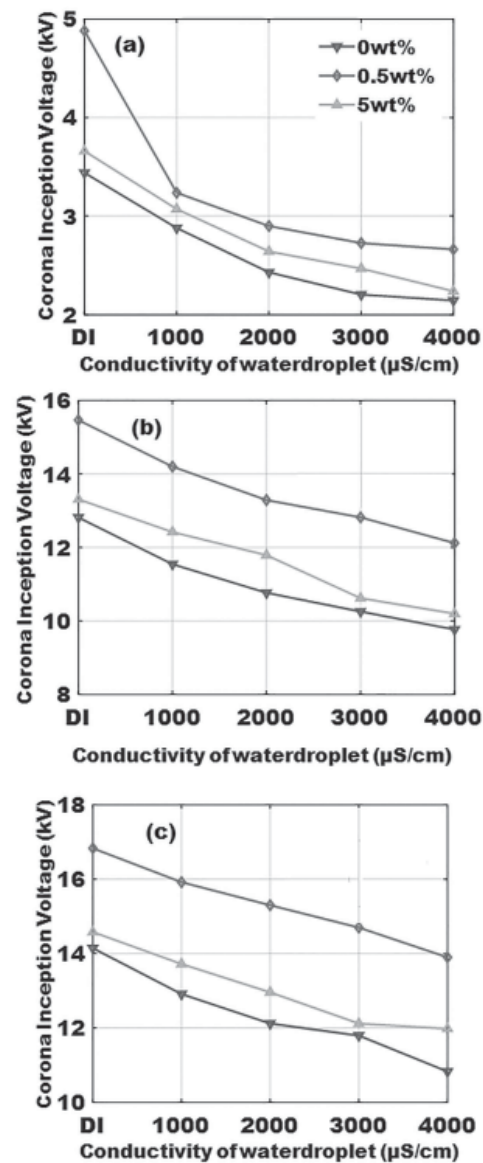


Figure 15 Variation in corona inception voltage due to water droplet with different conductivity on 5 wt% MoS<sub>2</sub> epoxy nanocomposites, (a) AC, (b) + DC, (c)-DC (DI-deionized water)

inception voltage is high under negative DC voltage compared to AC and positive DC voltage. The conducting water droplet will

easily get polarized and results in more stress at the triple point, leading to cause corona inception to occur at lower voltages. Under DC voltages, polarity dependency is observed with water droplet initiated corona inception voltage. Under positive DC voltage, the charges gets accumulated on the water droplet incepting corona discharge, at much lower voltage. Under negative DC voltage, the charge accumulates along electrostatic force, change the shape of water droplet to a filamentary shape. Such characteristic change in shape to occur and to incept corona discharge from thinned water droplet edge, higher negative voltage is required [20]. Figure 16 shows the damaged surfaces of nanocomposite due to arcing. It is realized that 0.5 wt% MoS<sub>2</sub> filled epoxy nanocomposite shows higher resistance to arcing than pure epoxy and other composites.

The UHF signal measured during corona discharge activity and its corresponding FFT is shown in Figure 17 (a) and (b) respectively. It is observed that the dominant frequency content of UHF signal formed is at around 0.9 GHz. To understand the dynamics of discharge activity/number of discharges and

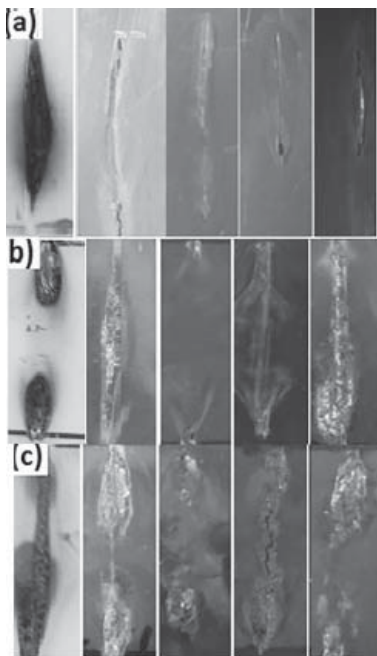


Figure 16 Damaged surfaces of epoxy nano composites due to arcing under (a) + DC, (b) -DC, (c) AC.

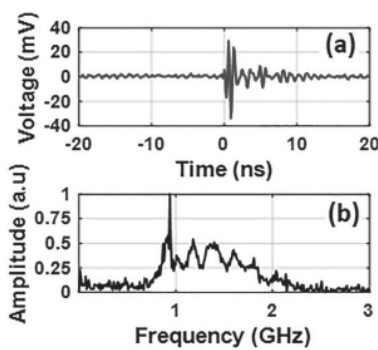


Figure 17 Typical (a) UHF signal, (b) its corresponding FFT due to corona discharge activity.

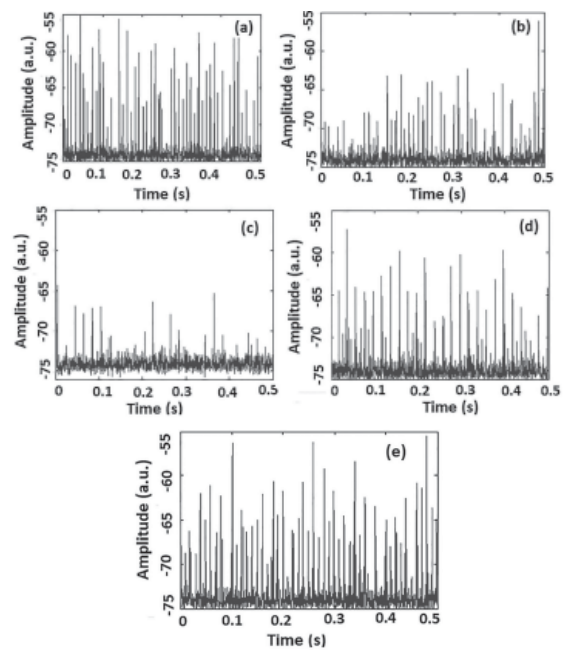


Figure 18 Spectrum analysis of corona discharge activity due to water droplets (i) pure, (ii) 0.25 wt%, (iii) 0.5 wt%, (iv) 1 wt%, (v) 5 wt%

magnitude of discharges occurrence during discharge activity process analyzed by use of UHF signal feeding it to an spectrum analyzer operating it in the zero span mode with 1 GHz as center frequency.

Figure 18 shows the spectrum analyzer pattern due to corona discharge initiated by water droplet present on the surface of the nanocomposite. It is observed that the number of discharges and their magnitude is less in 0.5 wt% of MoS<sub>2</sub> filled epoxy compared to unfilled epoxy and epoxy with another weight percentage of MoS<sub>2</sub>.

### 3.5 Transition Temperature Analysis

To understand the behavior of interactions between MoS<sub>2</sub> nanofiller and epoxy matrix, transition temperatures of all wt% of Epoxy/MoS<sub>2</sub> nanocomposites were measured. Figure 19 shows the DSC curves for epoxy/MoS<sub>2</sub> nanocomposites and Figure 20 shows the variations in  $T_g$  for all epoxy nanocomposites.

From Figure 20,  $T_g$  of nanocomposites increases with increase in wt% of MoS<sub>2</sub> up to 0.5 wt%, after which it reduces. In polymer

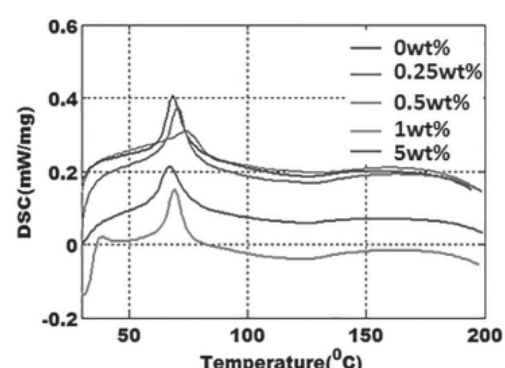


Figure 19 DSC curves for epoxy/MoS<sub>2</sub> nanocomposites.

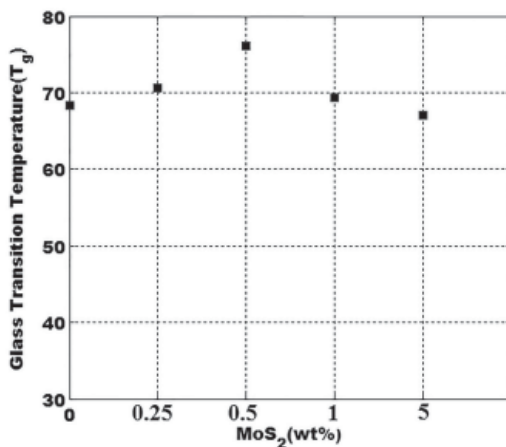


Figure 20 Variation in glass transition temperature with different percentages of MoS<sub>2</sub> in epoxy resin

nanocomposites, the interfacial interactions between the polymer and nanofiller have high influence on glass transition temperatures ( $T_g$ ), depending on its attractive or repulsive nature, which can increase or decrease [21]. In the present study, the increase in  $T_g$  at low filler loadings could be due to the interfacial interactions causing polymer chain immobility. Conversely, at high filler loadings, a decrease in transition temperature could be due to reduced interactions because of agglomerates.

### 3.6 Analysis of Discharges using OES

Figure 21 indicates the typical OES obtained during water droplet discharges for pure epoxy and 5 wt% epoxy/MoS<sub>2</sub> nanocomposite under positive DC voltage. The common elements

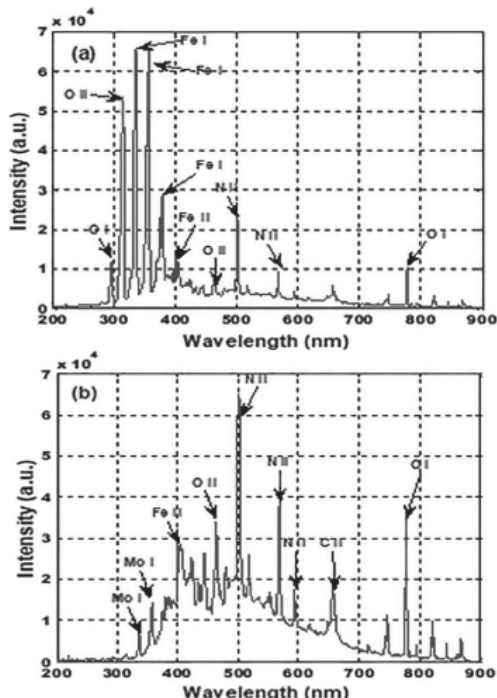


Figure 21 The typical optical emission spectrum of epoxy/MoS<sub>2</sub> nanocomposite during water droplet initiated discharge under DC voltage, (a) 0 wt%, (b) 5 wt%.

Table 1 Variation in plasma temperature with wt% of MoS<sub>2</sub>.

Wt% of MoS <sub>2</sub>	Plasma Temperature(K)
0	29076
0.25	26505
0.5	22464
1	22536
5	24605

found in both samples during plasma discharge are iron (Fe), oxygen (O) and nickel (Ni) and molybdenum peaks are found only in epoxy/MoS<sub>2</sub> nanocomposite, not in pure. Plasma temperature can be calculated using spectroscopic parameters, assuming local thermal equilibrium using Boltzmann-Saha equation.

$$T_e = 1.44 \frac{E_2 - E_1}{\ln \left[ \frac{I_1 \lambda_1 A_2}{I_2 \lambda_2 A_1} \frac{g_2}{g_1} \right]} \quad \dots \dots \dots (3)$$

Where  $E_1$  and  $E_2$  are excited energy levels,  $g_1$  and  $g_2$  are statistical weights of excited energy levels 1 and 2, respectively,  $A_1$  and  $A_2$  are transition probabilities of states,  $I_1$  and  $I_2$  are intensities of particular atomic species at  $\lambda_1$  and  $\lambda_2$  wavelength, respectively, and  $T_e$  is the plasma electron temperature under the condition of local thermodynamic equilibrium (LTE). Table 1 shows the plasma temperature of epoxy/MoS<sub>2</sub> nanocomposites. It is observed that discharge plasma temperature is lowest for 0.5 wt% MoS<sub>2</sub> added epoxy and it is 6612K less when compared with pure epoxy. The possible reason for it could be due to the increase in thermal conductivity of the epoxy/MoS<sub>2</sub> nanocomposites.

## 4 CONCLUSIONS

The important conclusions acquired based on the present study are the following.

- It is observed that surface discharge inception voltage of epoxy MoS<sub>2</sub> nanocomposite is high under DC voltage compared to AC voltages. Also above certain wt% of MoS<sub>2</sub> added to the epoxy resin reduces the SDIV.
- Measure of surface roughness near the surface discharge damaged zone is high with pure epoxy resin and when MoS<sub>2</sub> wt% is increased above certain limit. Also the measure of contact angle and SDIV have direct correlation. Dielectric constant and  $\tan \delta$  varies with wt% of MoS<sub>2</sub> in epoxy resin
- Corona inception voltage due to water droplet increases with increase in wt% of MoS<sub>2</sub> up to 0.5 wt%, above which marginal reduction is observed.
- It is observed that irrespective of the conductivity of water droplet, corona inception voltage is high for negative DC compared to AC and positive DC.
- 0.5 wt% MoS<sub>2</sub> filled epoxy nanocomposite has high resistance to discharges due to water droplets.
- Glass transition temperature ( $T_g$ ) of epoxy MoS<sub>2</sub> varies with filler loading.
- OES results indicate that the plasma temperature is low for epoxy resin with 0.5 wt% MoS<sub>2</sub>.
- In short, the results of the study indicates that by proper selection of nano filler added to base resin, it is possible to achieve required properties of the material, for power apparatus, in addition to compact insulation.

## References

- [1] Hackam R., "Outdoor HV composite polymeric insulators",

- IEEE Trans. Dielectr. Electr. Insul.*, **6**, 557-585 (1999).
- [2] Meyer L. H.; Cherney E. A.; and Jayaram S. H., "The role of inorganic fillers in silicone rubber for outdoor insulation-alumina tri-hydrate or silica", *IEEE. Electr. Insul. Mag.*, **20**, 13-21 (2004).
- [3] Eksik O.; Gao J.; Shojaee S. A.; Thomas A.; Chow P.; Bartolucci S. F.; Lucca D. A.; Koratkar N.; "Epoxy nanocomposites with two-dimensional transition metal dichalcogenide additives", *ACS Nano*, **8**, 5282-5289 (2014).
- [4] Wang X.; Xing W.; Xiaming F.; Lei S. Yuan H.; MoS<sub>2</sub>/Polymer Nanocomposites: Preparation, Properties, and Applications, *Polymer Reviews*, **57**, 440-466 (2017).
- [5] Li X.; Zhu H.; "Two-dimensional MoS<sub>2</sub> properties, preparation, and applications", *J.Materomics* 33-44 (2015).
- [6] Dissado L. A.; Fothergill J. C.; "Electrical Degradation and Breakdown in Polymers" London UK: Peter Peregrinus Ltd. 1992.
- [7] Karsten P.; Mikes E.; Isabelle H.; Gibleux T.; Treier Jean L.; "Evolution of high voltage gas insulated substations considering eco design aspects" CIGRE, B3-302\_2006
- [8] Tanaka T.; Matsuo Y.; and Uchida K.; "Partial Discharge Endurance of Epoxy SiC Nanocomposite", in 2008 Annual Report Conference on Electrical Insulation Dielectric Phenomena, 13, Quebec city, Canada (2008).
- [9] Espino-Cortes F. P.; Cherney E. A.; Jayaram S.; "Effectiveness of Stress Grading Coatings on Form Wound Start Coil Groundwall Insulation Under Fast Rise Time Pulse Voltages", *IEEE Trans. Energy Conversion*, **20**, 844-851 (2005).
- [10] Tremblay R.; Hudon C.; "Improved Requirements for Stress-Grading Systems at Hydro-Quebec", *Proc. Iris Rotating Machine Conference*, June 2007, San Antonio, TX, 6-10 (2007).
- [11] Tanaka T.; Yoshimichi O.; Ochi M.; Harada M.; Takahiro I.; "Enhanced Partial Discharge resistance of epoxy/clay nanocomposite prepared by newly developed organic modification and solubilization methods", *IEEE Trans. Dielectr. Electr. Insul.*, **15**, 81-89 (2008).
- [12] Crank J.; Mathematics of Diffusion, Oxford: Clarendon), 2nd Edition, 1975.
- [13] KozakoN.; Fuse Y.; Ohki T.; Okamoto and T. Tanaka, "Surface Degradation of Polyamide nanocomposites caused by partial discharges using IEC(b) Electrodes", *IEEE Trans. Dielectr. Electr. Insul.*, **1**, 833-839 (2004).
- [14] IEC publication, 60 112, "Recommended method for determining the comparative tracking index of solid insulating material under moist condition", (1972).
- [15] Judd M.D.; Yang L.; Hunter I.B.B.; "Partial discharge monitoring of power transformers using UHF sensors. Part I: sensors and signal interpretation", *IEEE Electr. Insul. Mag.*, **21**, 5-14 (2005).
- [16] Centurioni L.; Guastavino F.; Torello E.; "An investigation about the PD Degradation of Thin Polymer Films and its Correlation with Surface Charge Decay Measurements", *IEEE Electr. Insul. Conf.*, USA, 371-375 (2002).
- [17] Choi J.; Zhang, H.; Du, H.; Choi J. H.; Understanding Solvent Effects on the Properties of Two-Dimensional Transition Metal Dichalcogenides. *ACS Appl. Mater. Interfaces*, **8**, 8864-8869 (2016).
- [18] Zhang, L.D.; Zhang, H.F.; Wang, G.Z.; Mo C.M.; Zhang, Y.; "Dielectric behavior of nano-TiO<sub>2</sub> bulks", *Phys. Stat. Sol.*, **157**, 483-491 (1996).
- [19] Ciuprina, F.; Plesa, I.; Notinger P.V.; Tudorache T.; Panaitescu D.; "Dielectric properties of nanodielectrics with inorganic fillers", *Annual Report Conference on Electrical Insulation and Dielectric Phenomena (CEIDP)*, Quebec, October (2008).
- [20] Higashiyama Y.; Shiho Y.; and Toshiyuki S.; "DC corona discharge from water droplets on a hydrophobic surface", *J.Electrostatics*, **55**, 351-360, (2002).
- [21] Ash B. J.; Schadler L. S.; W.Siegel R.; "Glass transition behavior of Alumina / poly methyl methacrylate nanocomposites", *Materials Letters*, **55**, 83-87 (2002).